

Supporting Information. Starko, Samuel, Christopher J. Neufeld, Lianna M. Gendall, Brian Timmer, Lily Campbell, Jennifer Yakimishyn, Louis Druehl, and Julia K. Baum. Microclimate predicts kelp forest extinction in the face of direct and indirect marine heatwave effects. *Ecological Applications*.

Appendix S1

Supplemental Tables

Table S1. Summary of historical kelp distribution sources used in this study. Bolded data types were quantitatively compared to modern resurveys.

Data type	Date	Coverage	Publication or data source
Hand drawn map	July 1971	Trevor Channel (South and North)	Sharp 1974
Shoreline surveys	mid-1970s ¹	Trevor Channel (South and North)	Druehl <i>et al.</i> 1978
Aerial image (high elevation)	July 7 1981	Trevor Channel (North only)	Province of British Columbia
Parks Canada subtidal boat surveys	June - Aug 1993. June – Aug 1994, June – Aug 1995	Trevor Channel and Broken Group Islands	Druehl & Elliot 1996 Parks Canada surveys
Parks Canada intertidal surveys	June - Aug 1993. June – Aug 1994, June – Aug 1995	Trevor Channel and Broken Group Islands	Druehl & Elliot 1996 Parks Canada surveys
Aerial flyover (low elevation)	Aug 2007	Trevor Channel (South only)	ShoreZone initiative
BMSC student kelp forest maps	Aug 2008	Trevor Channel (North only)	BMSC 2008 summer student project
Satellite imagery	Oct 2013 May 2016	Trevor Channel (South only)	Google Earth Pro
Aerial image (high elevation)	Jul 2014	Trevor Channel	Province of British Columbia

¹Exact date not recorded but survey conducted during the summer (June – Aug)

Supplemental Figures

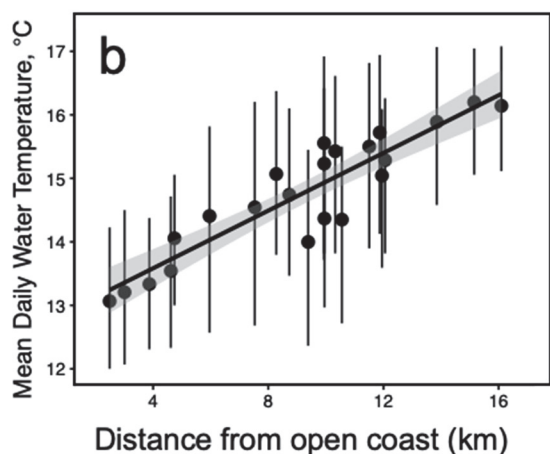
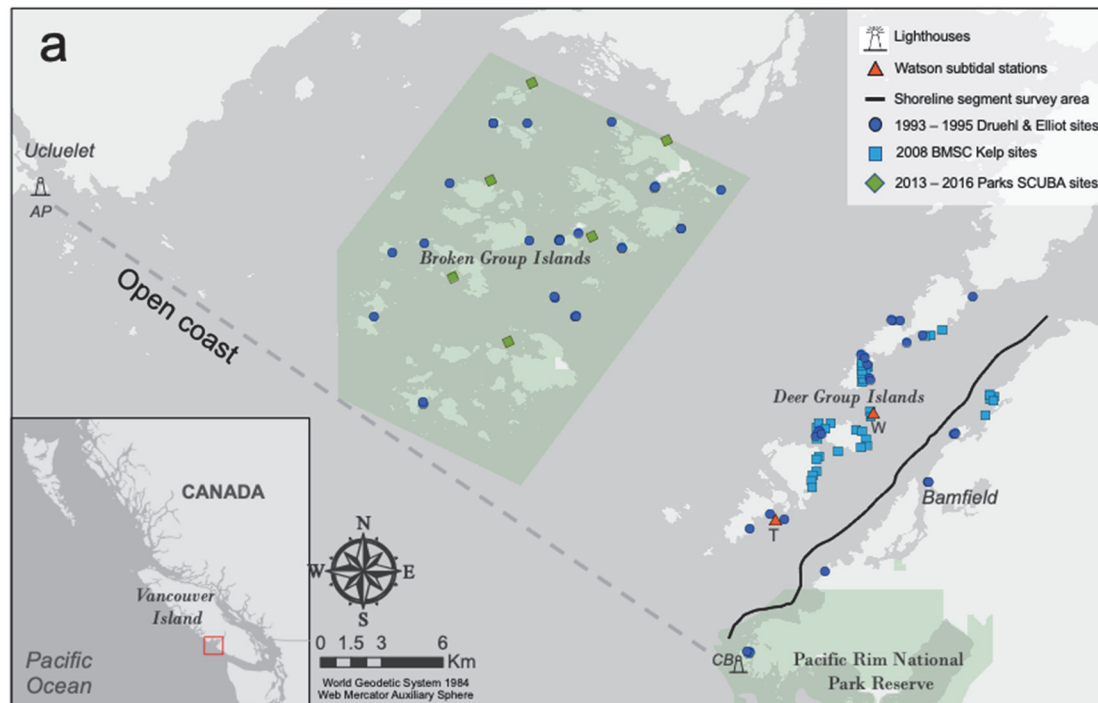


Fig. S1. Study region and spatial variation in temperature. Our study region (a) included two major island groups as well as coastline on mainland Vancouver Island. The Broken Group Islands and the south end of our mainland Vancouver Island region are part of Pacific Rim National Park. With increasing distance from the open coast (denoted by dotted line), sea surface temperatures increase (b) Error bars in panel b indicate mean daily maximum and mean daily minimum, while the point indicates mean daily average temperature. Temperature measurements were taken at sites ($n = 22$) along the shoreline segment survey area as well as in the Deer Group Islands. CB = Cape Beale; AP = Amphitrite Point. Distance from open coast was measured as the distance from the dotted line between CB and AP.

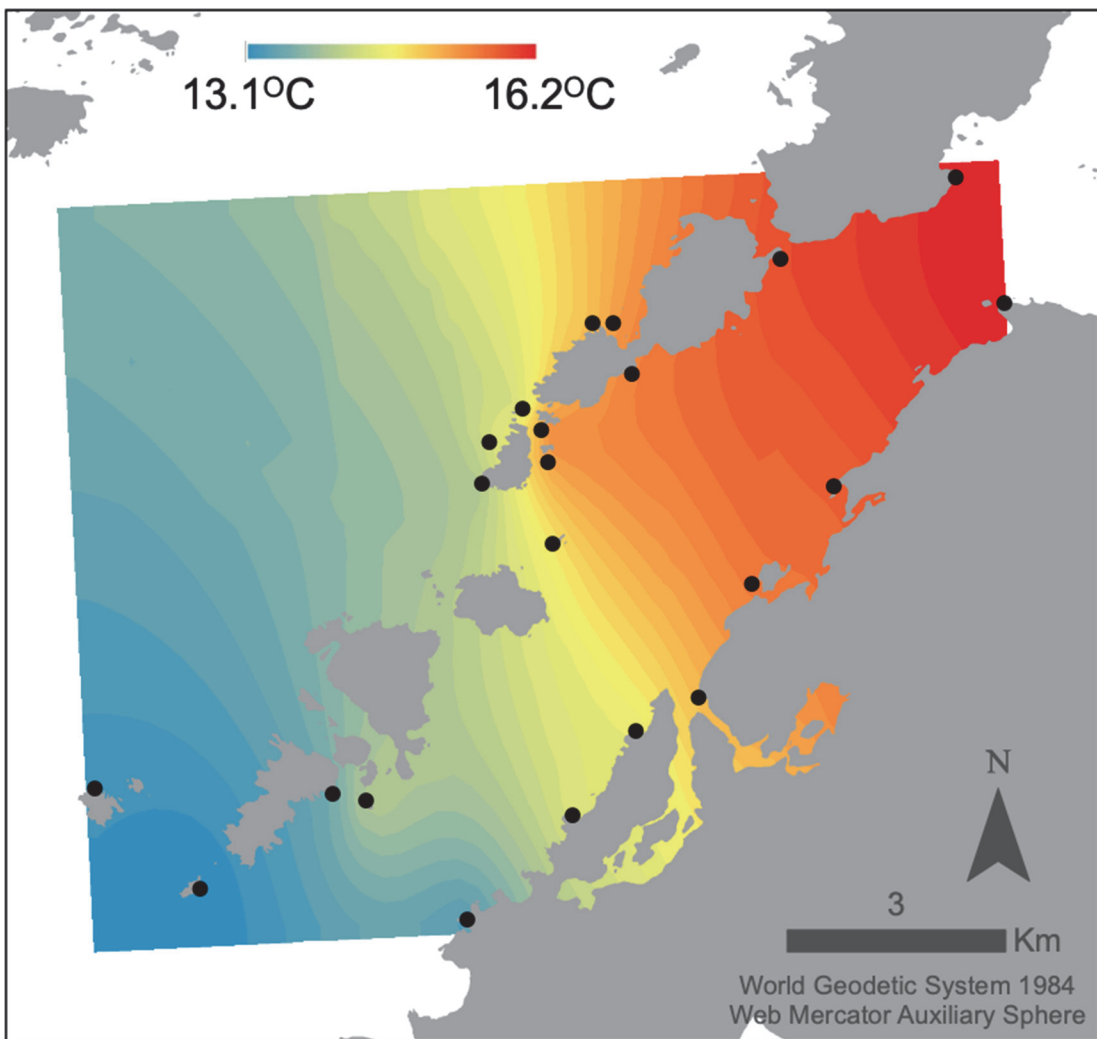


Fig. S2. Spatial variation in summer average water temperatures across southeast Barkley Sound. Sites (n=22) where temperature were measured *in situ* in 2019 are shown as black dots. Mean water temperature is interpolated using Ordinary Kriging (exponential variogram fit).

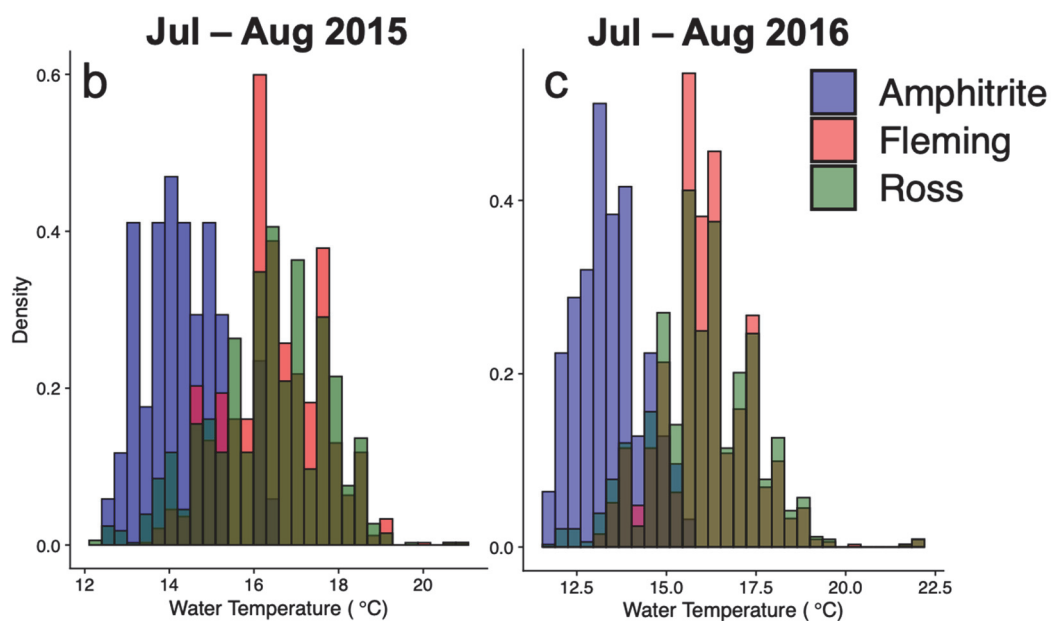
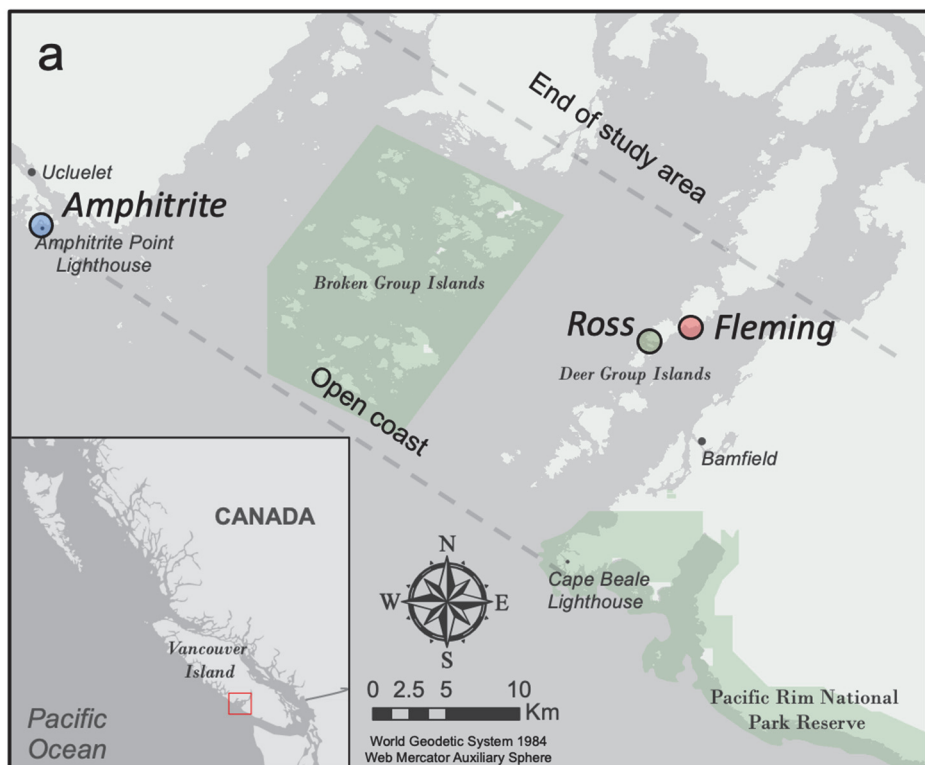


Fig. S3. In situ surface temperatures from the heatwave at inshore relative to outer shore sites. (a) A map showing the locations of three sites with in situ temperature during the 2014-2016 marine heatwave. (b-c) The distribution of temperature measurements taken at Amphitrite Point versus inshore sites in the summer of 2015 (b) and 2016 (c).

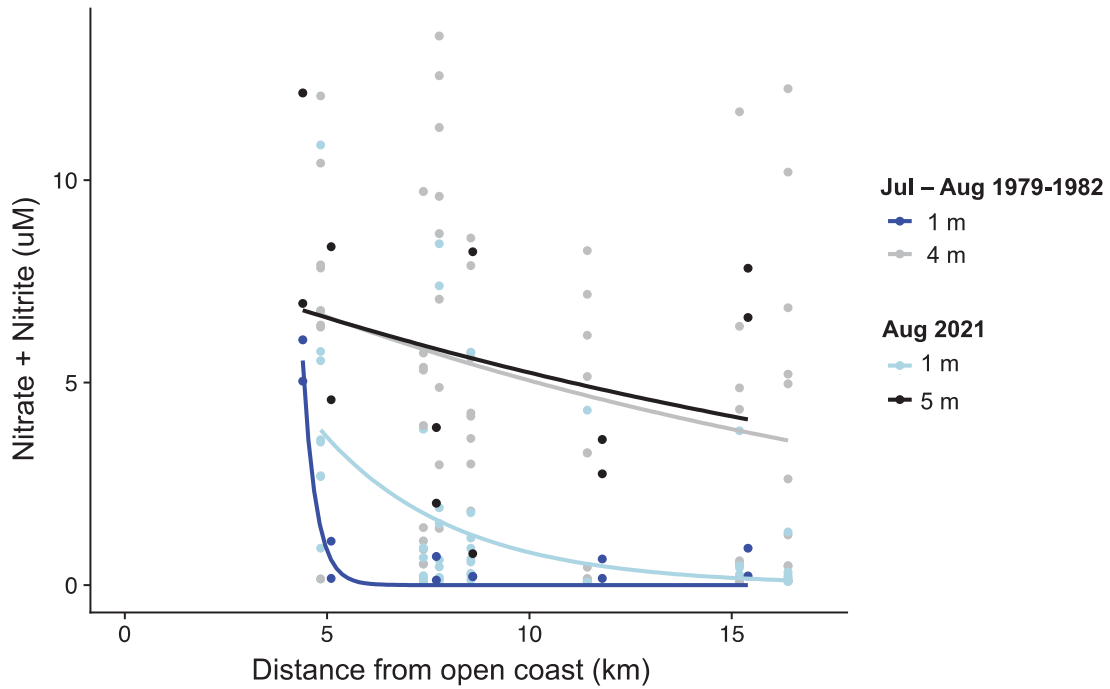


Fig S4. Dissolved nitrogen (nitrate + nitrite) versus distance from open coast. Data points represent individual water samples taken in July or August. Colours indicate timeframe and/or depth. Non-linear models ($y = ae^{-bx}$) are fit to the data separately, reflecting a negative relationship between dissolved nitrogen and distance from open coast. Parameter estimates and supporting statistics are as follows: 1979-1982 – 1m ($a = 16.539$, $t = 1.818$, $p = 0.074$; $b = 0.302$, $t = 3.352$, $p = 0.001$); 1979-1982 – 4m ($a = 8.688$, $t = 4.182$, $p < 0.001$; $b = 0.05$, $t = 2.124$, $p = 0.038$); 2021 – 1m ($a = 512200$, $t = 0.26$, $p = 0.8$; $b = 3.12$, $t = 3.581$, $p = 0.005$); 5m ($a = 8.312$, $t = 2.391$, $p = 0.037$; $b = 0.046$, $t = 0.919$, $p = 0.380$).

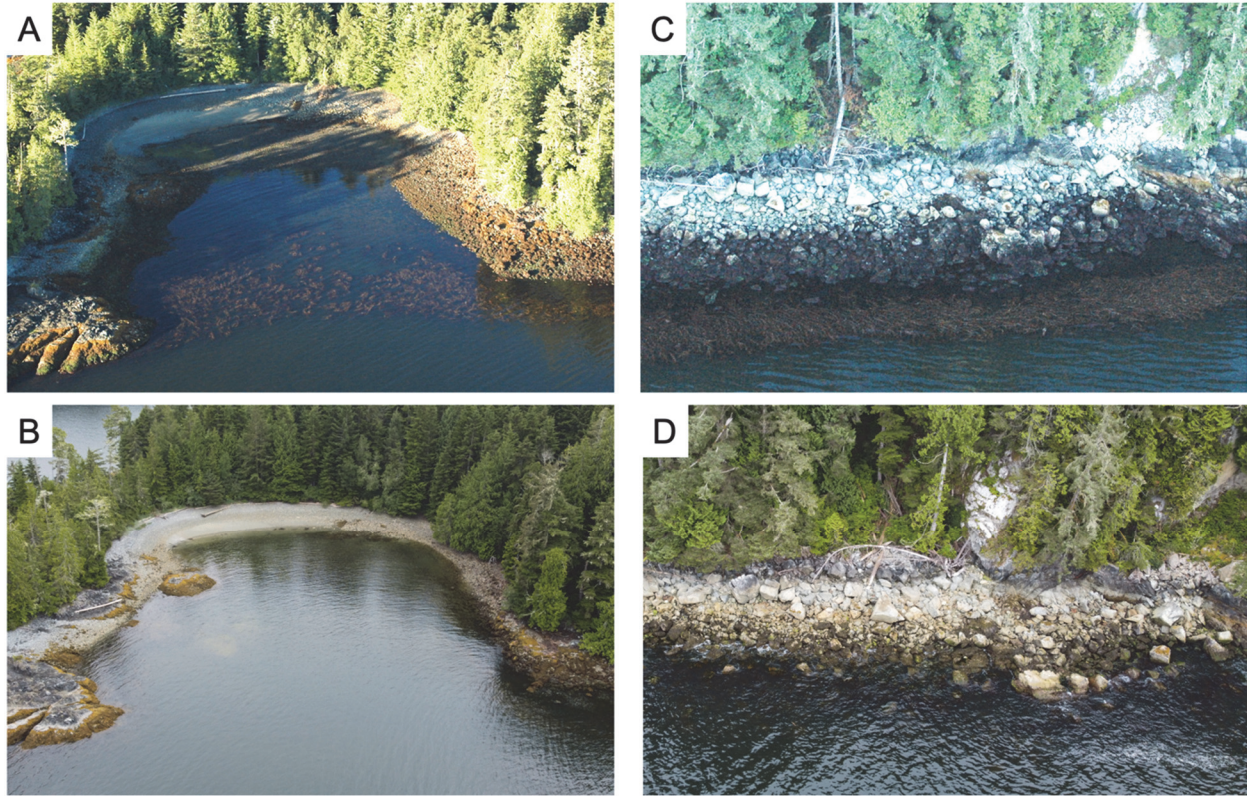


Fig. S5. Loss of *Macrocystis* forests around Dixon Island (a -b) and North of Roquefoil Bay (c – d). Photos in panels A, C were taken during the 2007 ShoreZone flyover while photos in panels B,D were taken in 2020 using a UAV. Note that the Dixon Island forest was not replaced by an urchin barren. While some urchins were present in the shallows, this area is largely boulder, cobble and sand with “understory” kelp (e.g., *Neoagarum*, *Saccharina*) still present along the bottom (see Supp Results).



Fig. S6. Loss of *Nereocystis* forest at Helby Island. Photos were taken in August 2010 (a) and August 2019 (b).

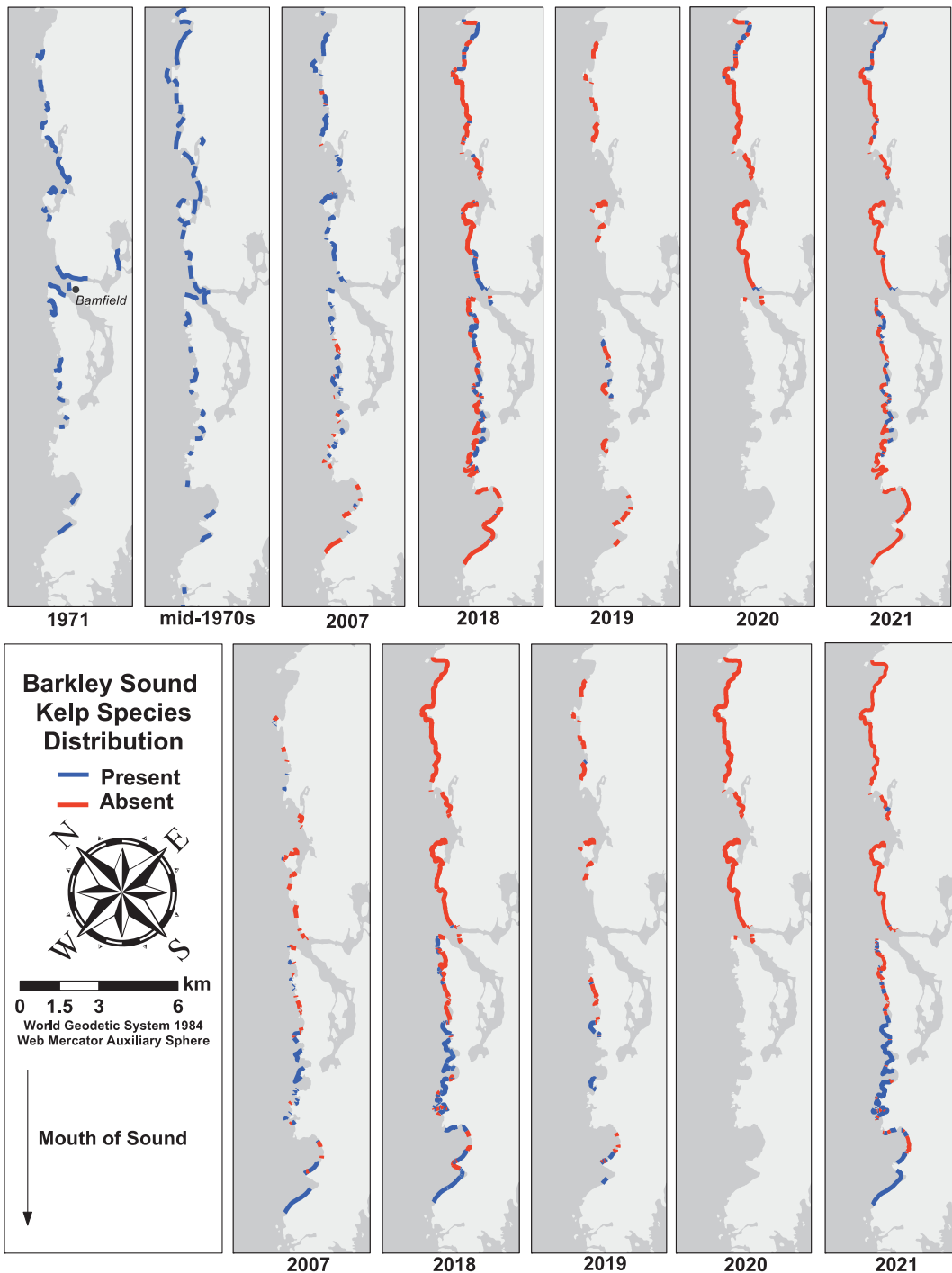


Fig. S7. The distribution of canopy forming kelp species, *Macrocystis pyrifera* (top row) and *Nereocystis luetkeana* (bottom row), along the SE wall of Barkley Sound. Data from 1971 and the mid-1970s are adopted from hand-drawn maps. All other years represent data from shoreline segments (see Table S1). Stretches of shoreline not colored in blue or red were not surveyed in a given year.

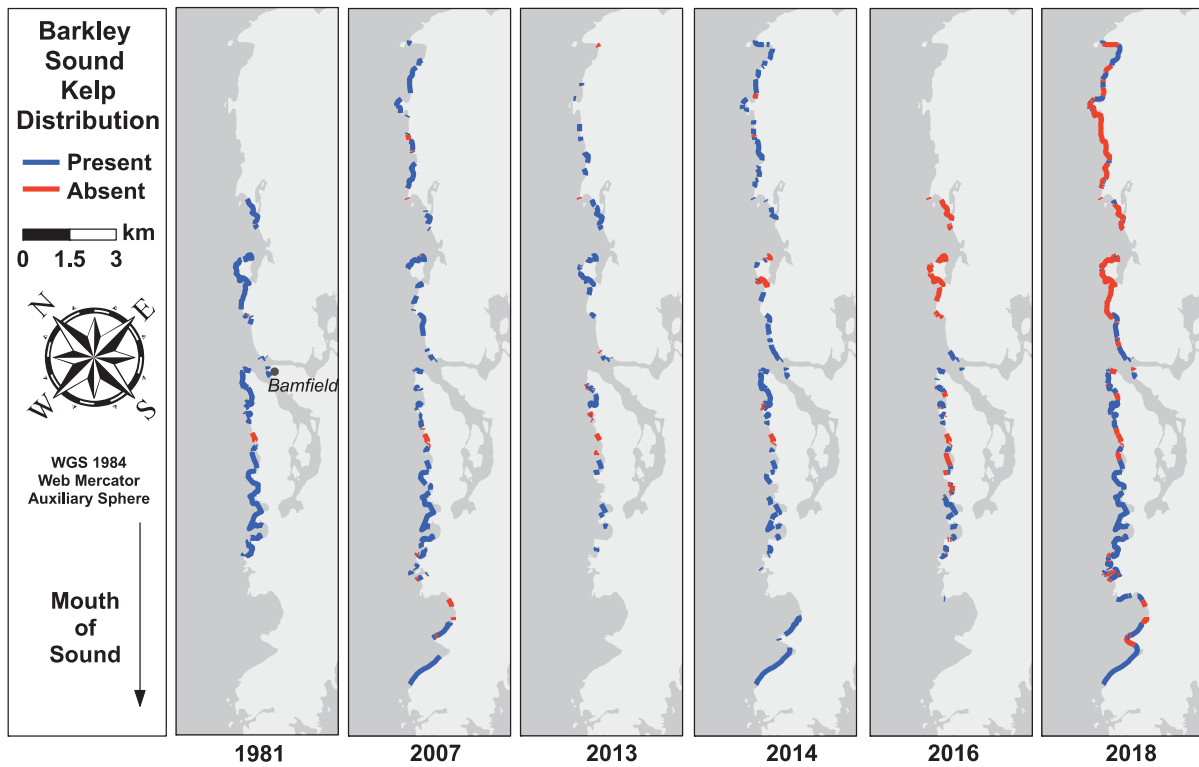


Fig. S8. The distribution of canopy forming kelp species (not distinguished by species) along the SE wall of Barkley Sound. Data are from shoreline segments (see Table S1) but represent primarily surveys where species could not be discerned. 2007 and 2018 are included for comparison with data for both species pooled. Stretches of shoreline not colored in blue or red were not surveyed in a given year.

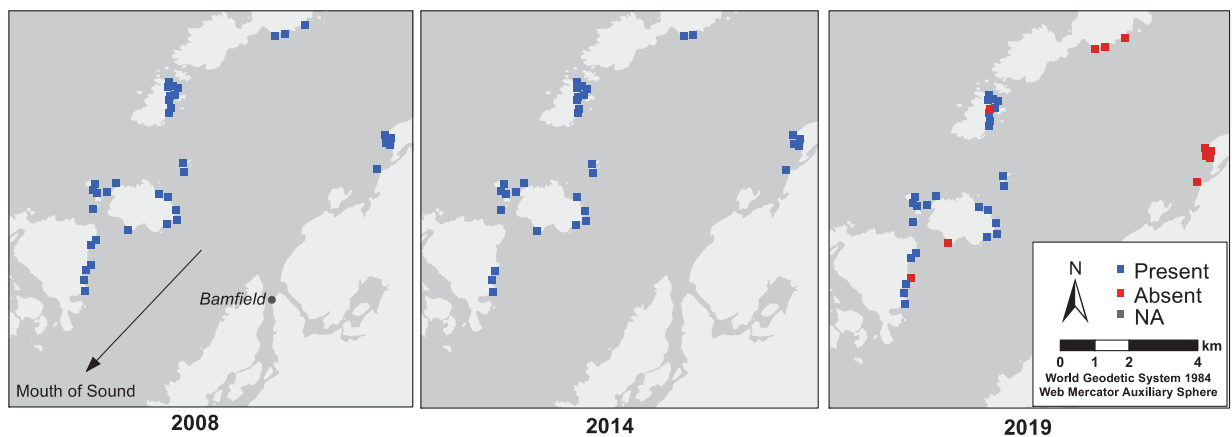


Fig. S9. Locations of *Macrocystis* kelp forests initially recorded in a 2008 BMSC student report. Shown are the original survey data (2008), occurrence data at these same forests from aerial imagery (2014) and resurveys of these forests in 2019. Presence-absence of forests are indicated by colour.

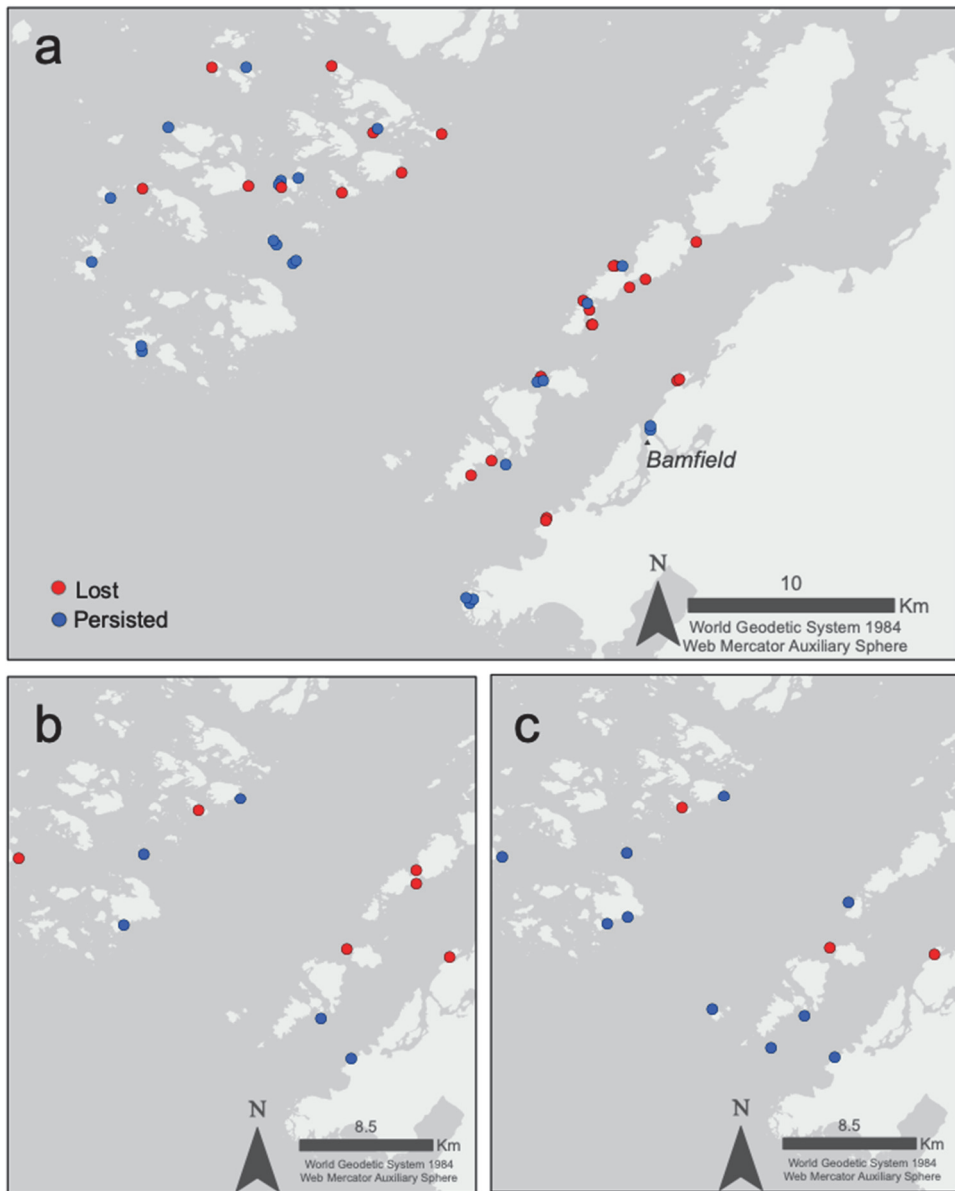


Fig. S10. Results of resurveys conducted at intertidal (a) and subtidal (b-c) sites established in 1993-1995. Panels a,b show results from resurveys of *Macrocystis pyrifera*, while panel c shows data on *Nereocystis luetkeana*.

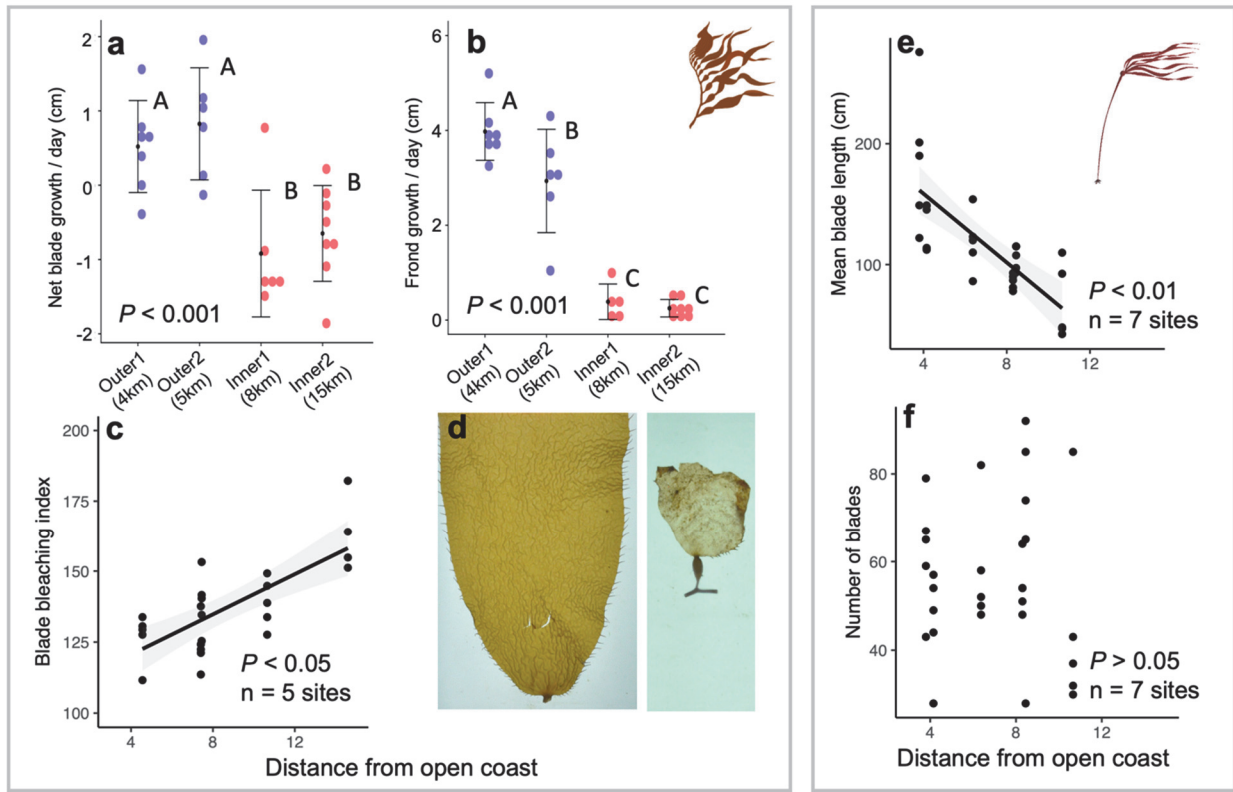


Fig. S11. Growth rate and condition metrics of canopy kelps along an environmental gradient of temperature and nutrients. *Macrocystis pyrifera* (a-d) and *Nereocystis luetkeana* (e,f). Each panel shows a given metric of growth or condition plotted against distance from the open coast. Linear models are shown in black with standard error shown in grey. Panel d shows examples of two blades both growing at the surface but at different sites: Second Beach, ~4.5 km from open coast (left) and Nanat Bay, ~15km from open coast (right).

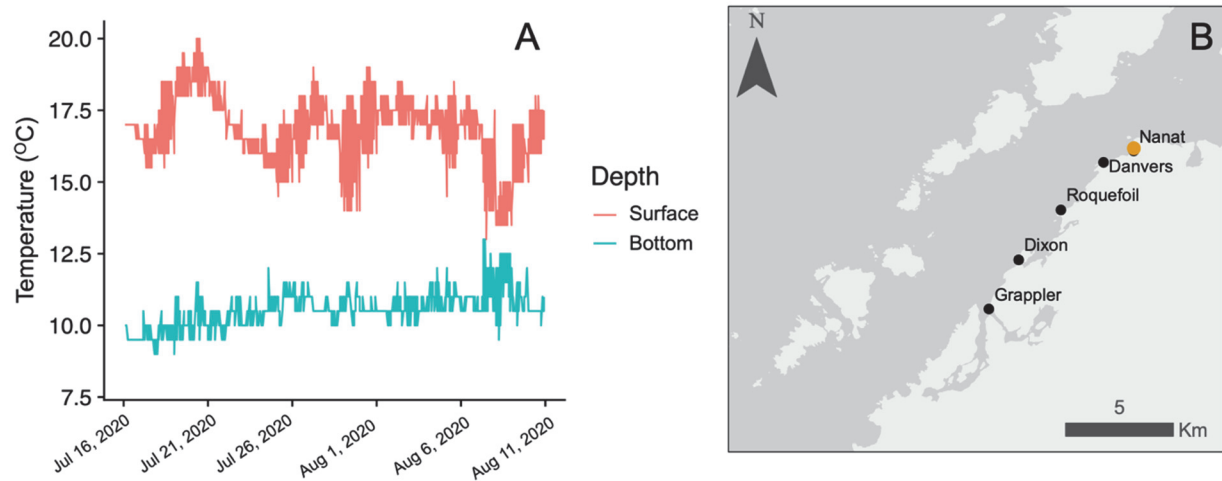


Fig. S12. Depth profiles from the summer of 2020 at Nanat Bay. Panel A shows the temperatures recorded by iButton loggers attached to a floating buoy anchored at ~8m depth. The surface logger was placed at 0.1m below the surface, while the bottom logger was located at 0.5m above the bottom (and therefore actual depth varies with tide). Panel B shows the location of temperature logger buoys deployed in 2020 with the location of the Nanat buoy shown in orange.

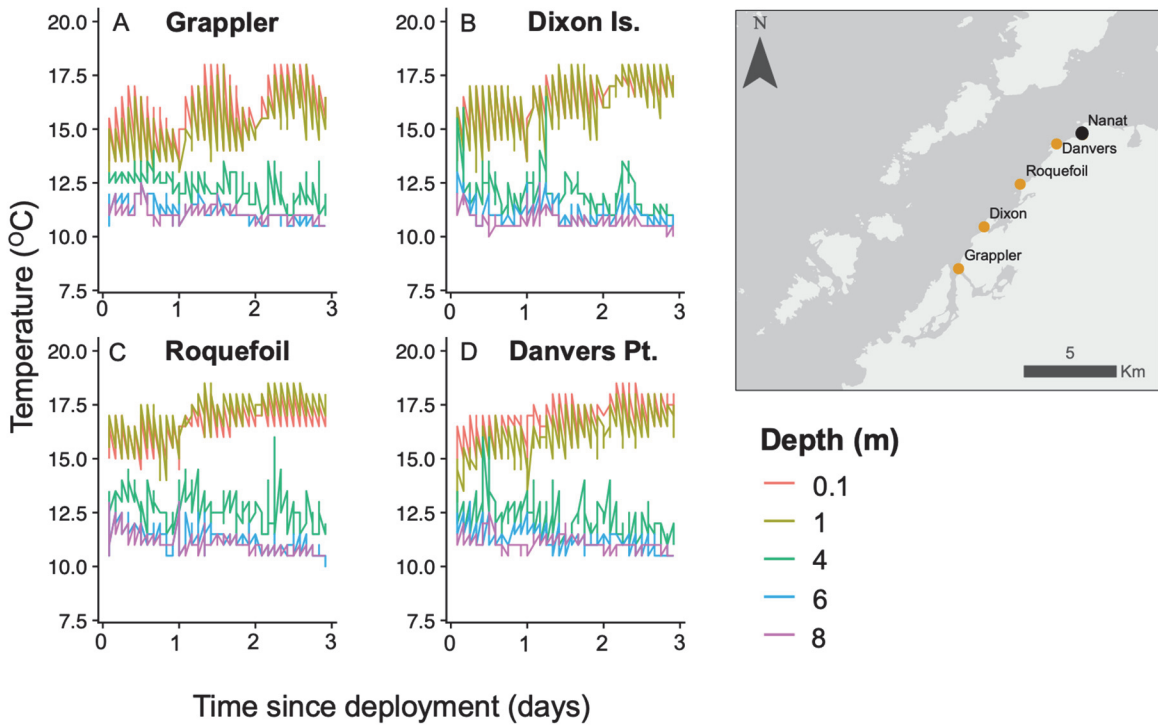


Fig. S13. Depth profiles from the summer of 2020 at four sites north of Bamfield. Panels A–D shows the temperatures recorded by iButton loggers attached to a floating buoy anchored at $\sim 10\text{m}$ depth. Loggers were suspended from the buoy at depths of 0.1 – 8m below the surface (and did not vary in depth with tide). Panel E shows the location of temperature logger buoys deployed in 2020 with the location of these four buoys shown in orange.

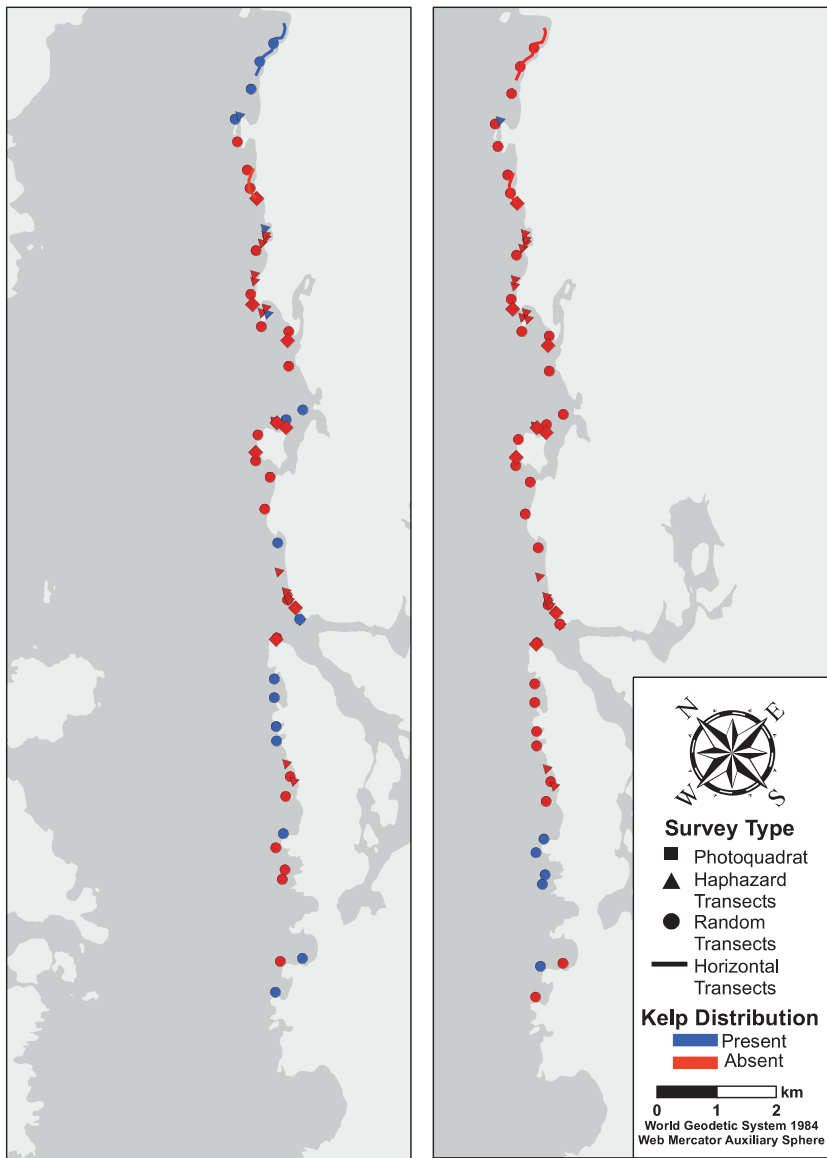


Fig. S14. Location of ROV surveys and photoquadrats conducted along the SE wall of Barkley Sound, showing the distribution of both kelp species detected in these surveys.
 Shown are data from both random transects, which were formally analyzed (see Fig 4 in main text), and haphazard transects which were conducted to better characterize the distribution of submerged kelp forests. Left = *Macrocystis*; Right = *Nereocystis*.

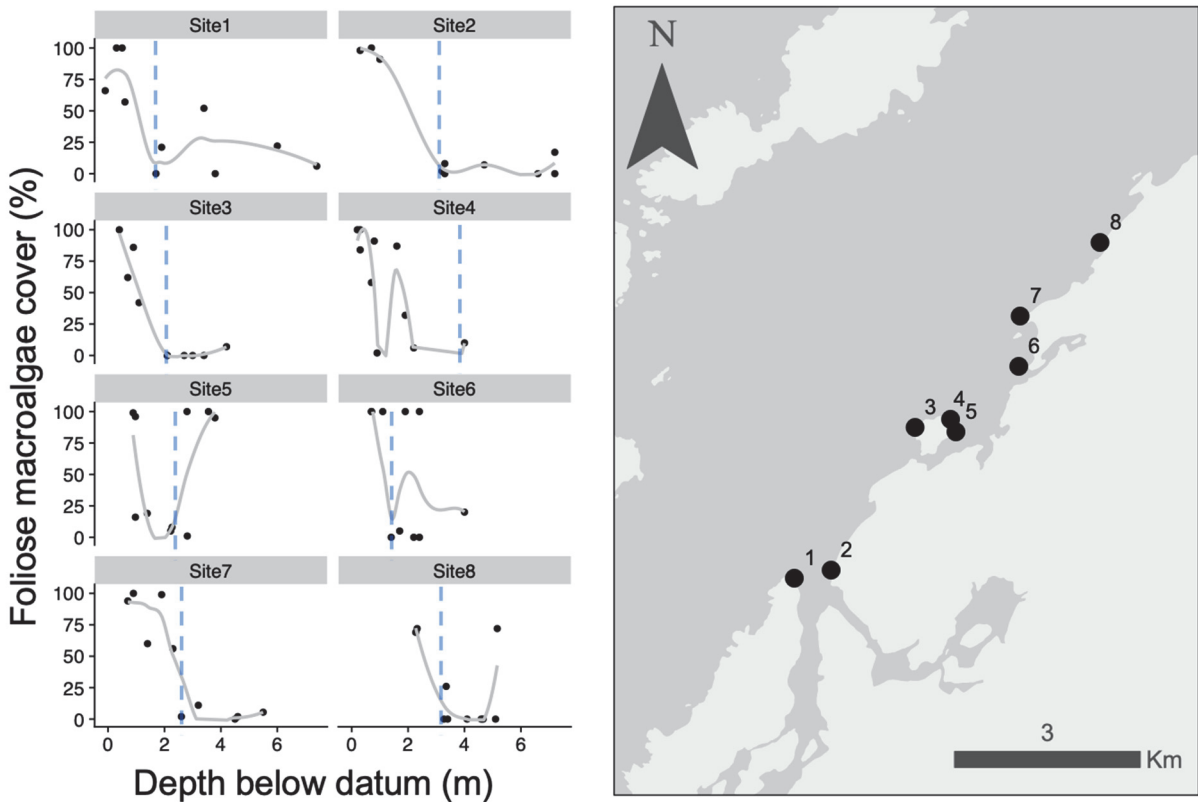


Fig. S15. Percent cover of non-canopy forming macroalgae at sites ($n = 8$) from which kelp forests were lost. Panels on the left show the percent cover of all foliose macroalgae versus depth as measured using photoquadrats. The blue vertical line indicates the shallowest depth at which urchins were captured by the photoquadrat. The righthand panel shows the location of all 8 sites.

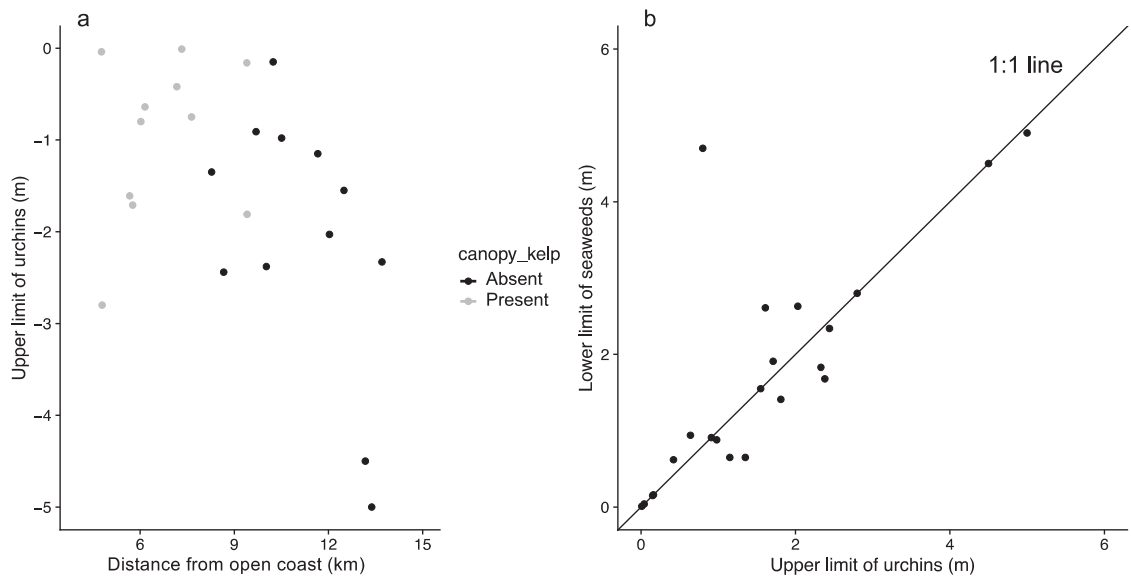


Fig S16. Vertical distribution of urchins and macroalgae along the shore. In panel a, the outliers are from sites that are exceptionally steep and moderately wave exposed, allowing macroalgae to extend deeper than is typical. Sites without urchins (e.g., sandy sites) are excluded. In panel b, the outlier is a result of sandy, urchin-free habitat below the main rocky reef at the site. All depths are below chart datum.

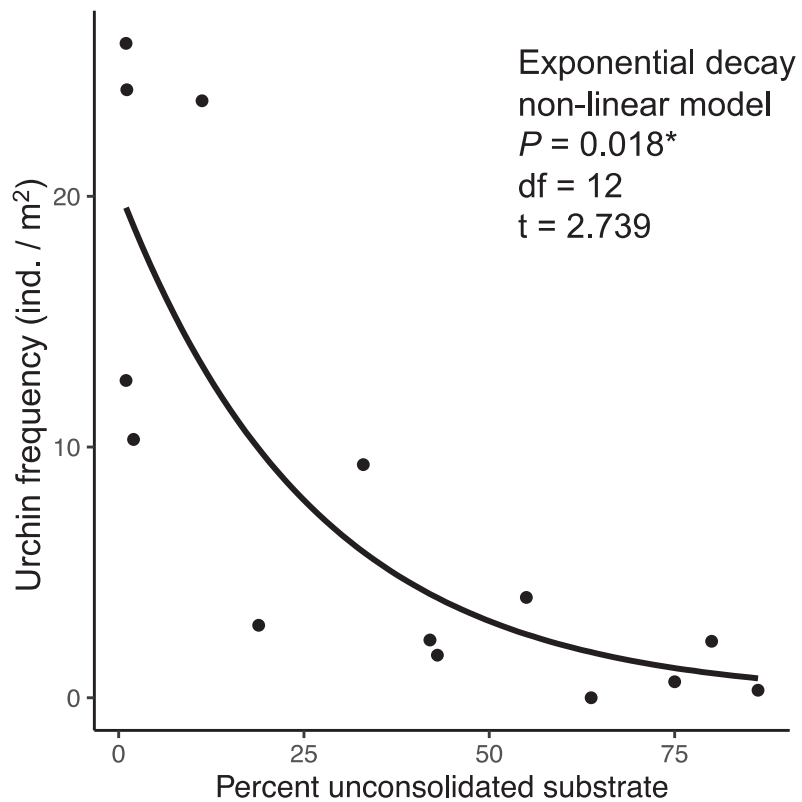


Fig. S17. Urchin density declines with increasing sand, sediment or cobble (unconsolidated substrate). These data are from photoquadrat surveys conducted at the edge of kelp forests, where remnant kelp forests further from the open coast are primarily located on unconsolidated substrate.

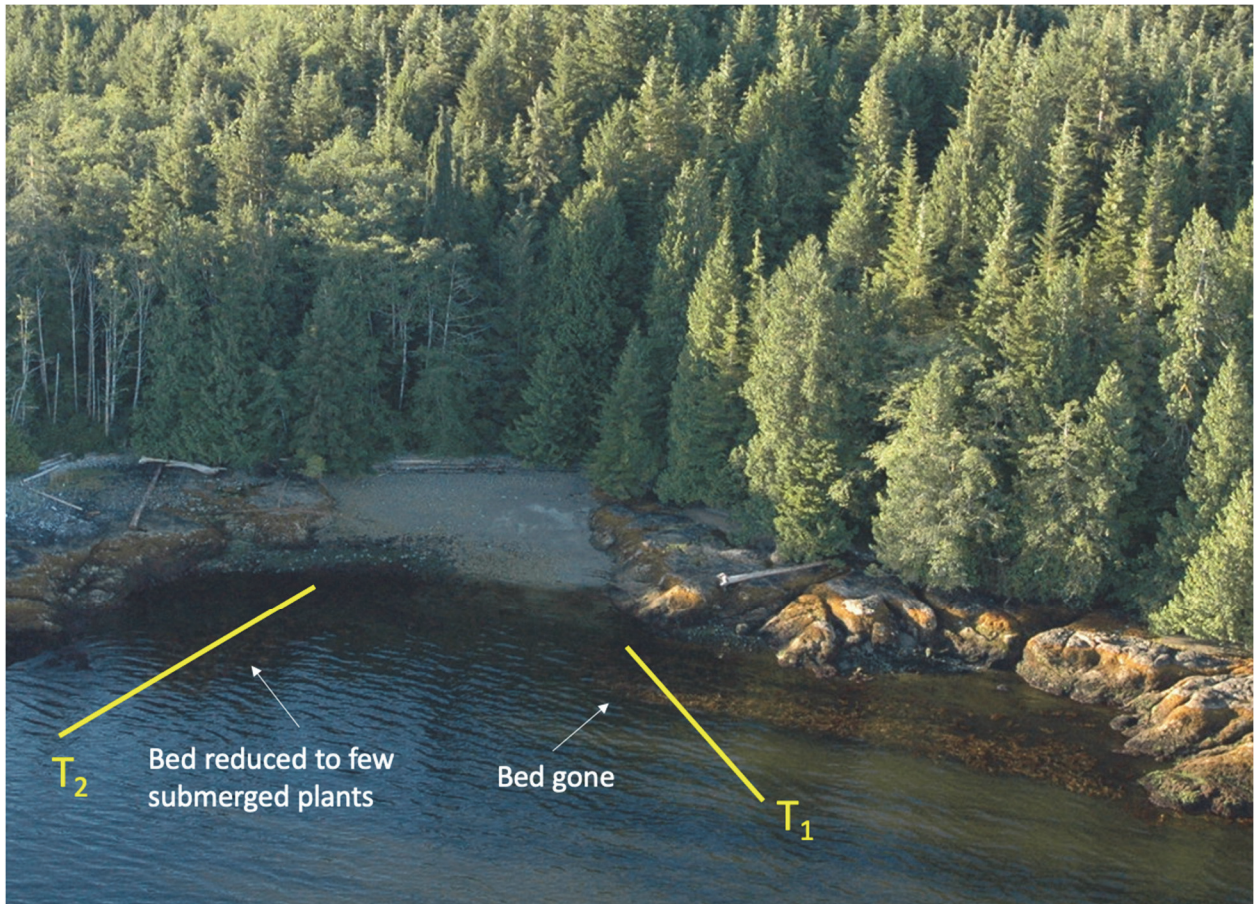


Fig S18. ROV surveys conducted in a small cobble bay north of Roquefoil Bay overlaid on image from 2007. Two transects ROV were conducted at this site and neither showed signs of urchin overgrazing. Kelp forests shown here have been largely replaced by understory kelp or brown algae (e.g., *Desmarestia* spp.). A small number of individuals were found in T₂ showing signs of physiological stress and none reached the surface in 2020.

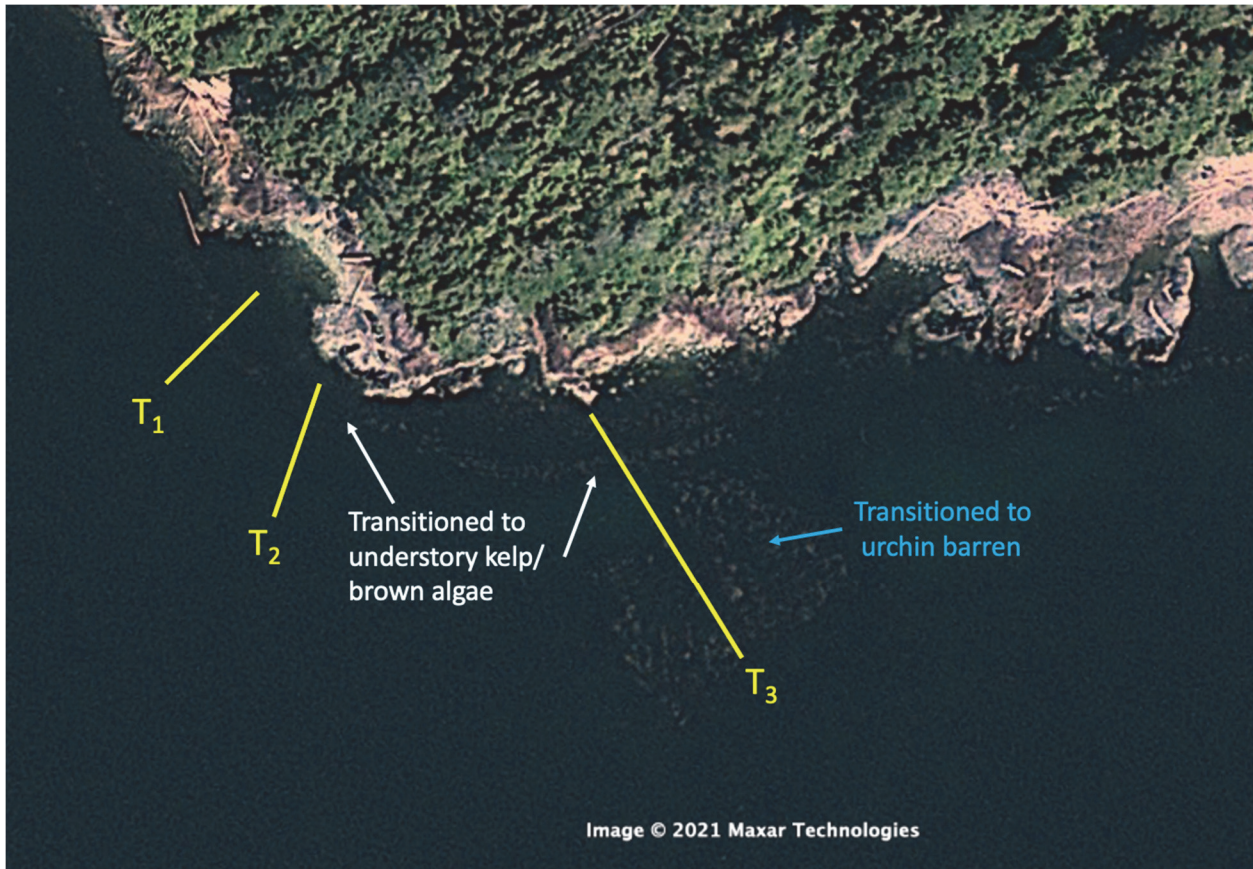


Fig. S19. ROV surveys conducted on the South side of Fleming Island in 2020 overlaid on image from 2013. No urchins were seen during transect 2, while only one small patch of urchins was seen during transect 2 (on a boulder surrounded by kelp). Transect 3 revealed that the offshore reef shown in the photo has transitioned to an urchin barren and is occupied by urchins, while the fringing bed has been replaced by prostrate kelps and *Desmarestia* and lacked urchins. Image courtesy of Google Earth Pro.

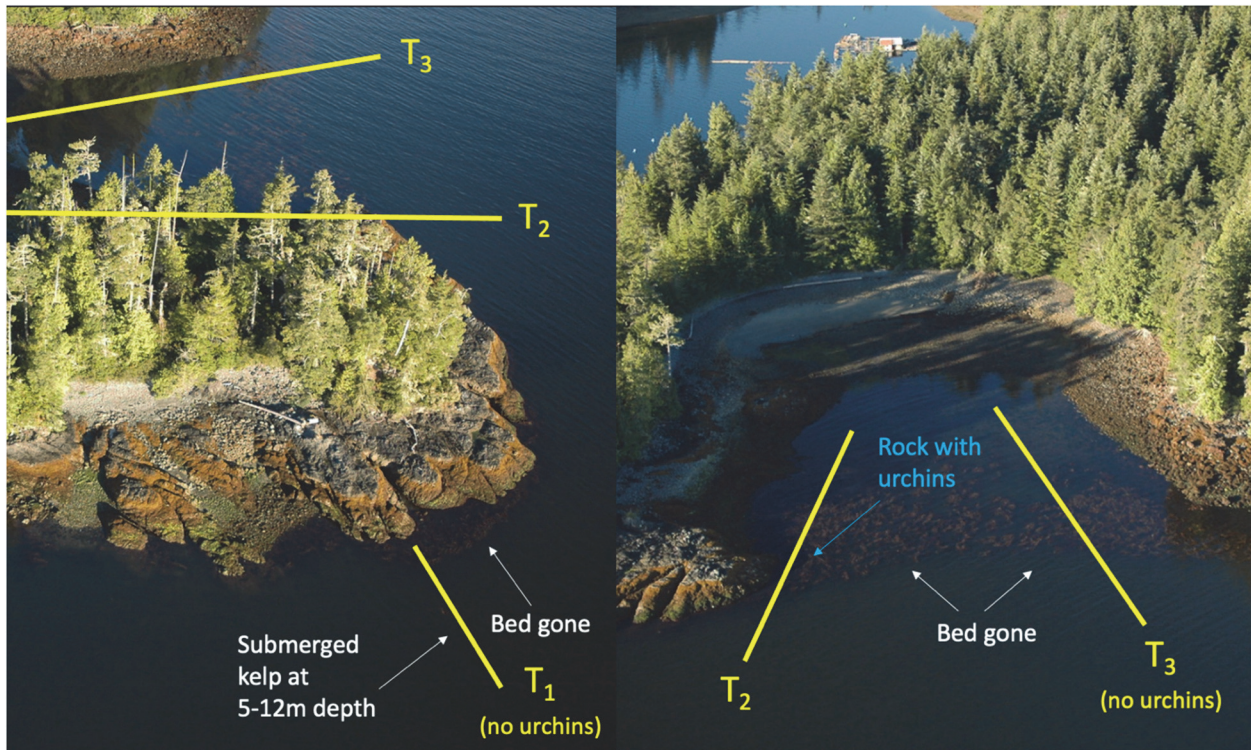


Fig. S20. ROV surveys conducted on the north side of Dixon Island overlaid on image from 2007. We conducted three transects in this area (T₁ was a random transect while T₂ and T₃ were haphazard surveys). T₁ and T₂ revealed no urchins but both lacked upright *Macrocystis* entirely. T₃ also generally lacked urchins, except for a large boulder on which we found four urchins. A submerged kelp bed was found between 5-12m at this site.

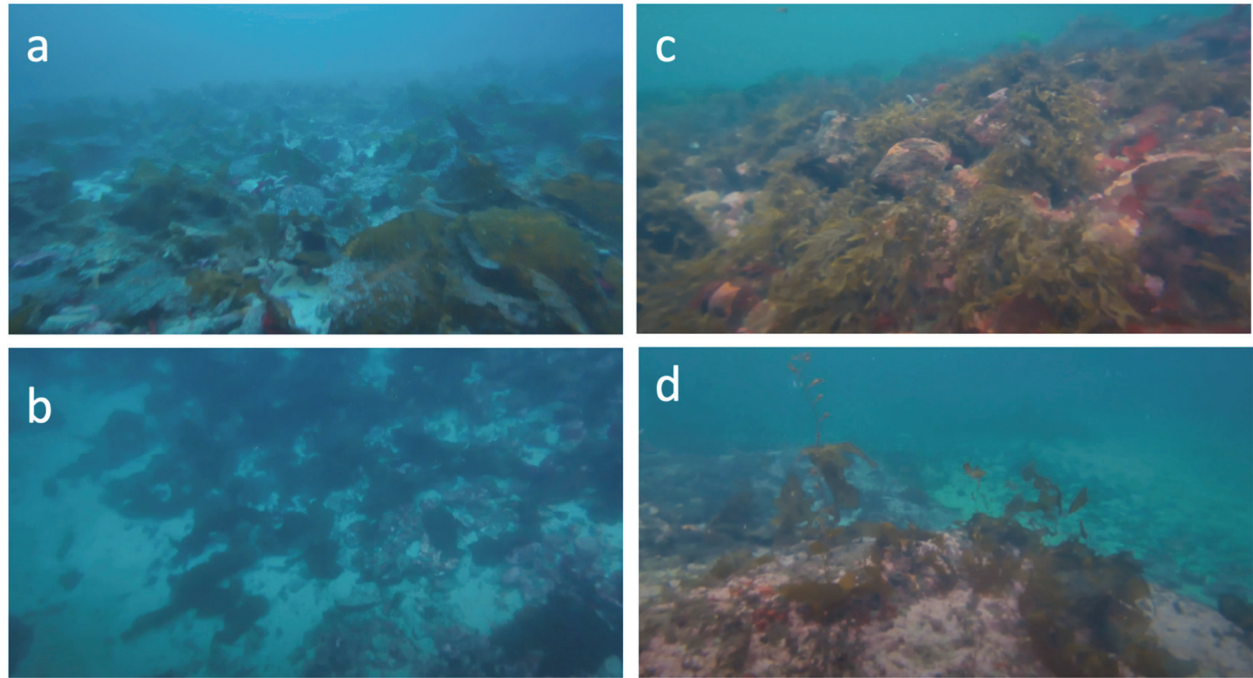


Fig. S21. Examples of subtidal macroalgae communities in locations with few to no urchins that have lost canopy-forming kelp forests. (a, b) An understory kelp forest (primarily *Neoagardum fimbriatum*). (c) *Desmarestia* on boulders found ~1-2m below datum at many sites. (d) A submerged patch of *Macrocystis* (not prostrate form) showing signs of canopy die-back. Photos taken during ROV surveys in October 2020.

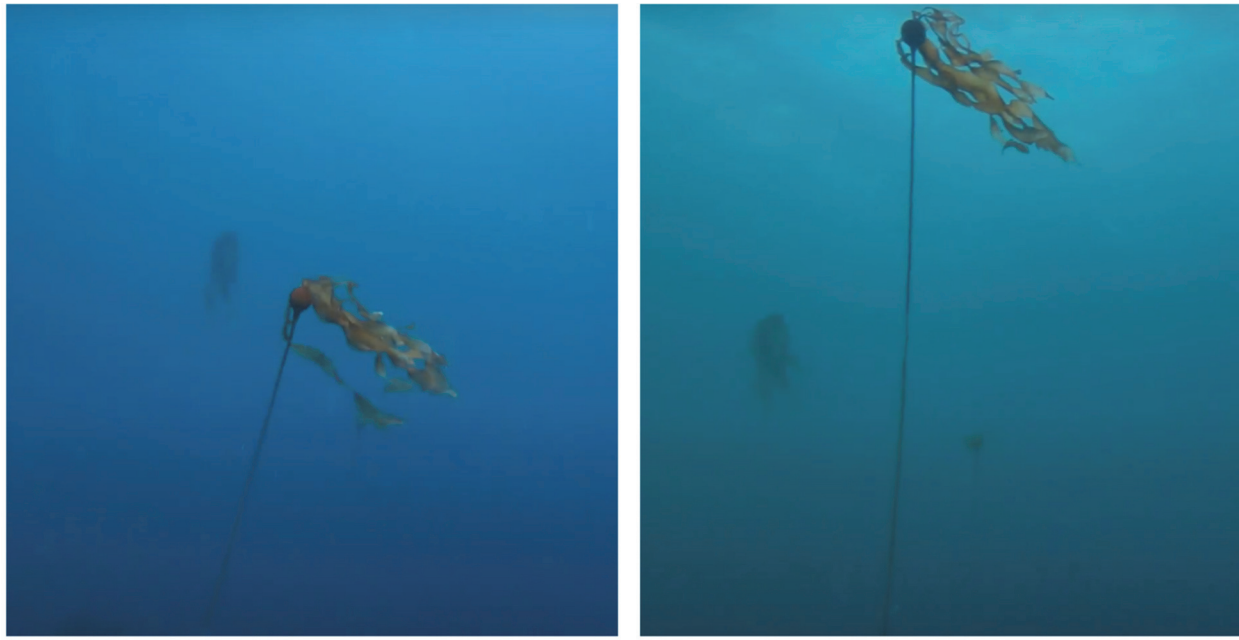


Fig. S22. *Nereocystis* individuals found at a far inshore site that were ~3-5m below datum and showed signs of physiological stress. Photos taken during ROV surveys in October 2020 but this pattern was also observed earlier in the summer.

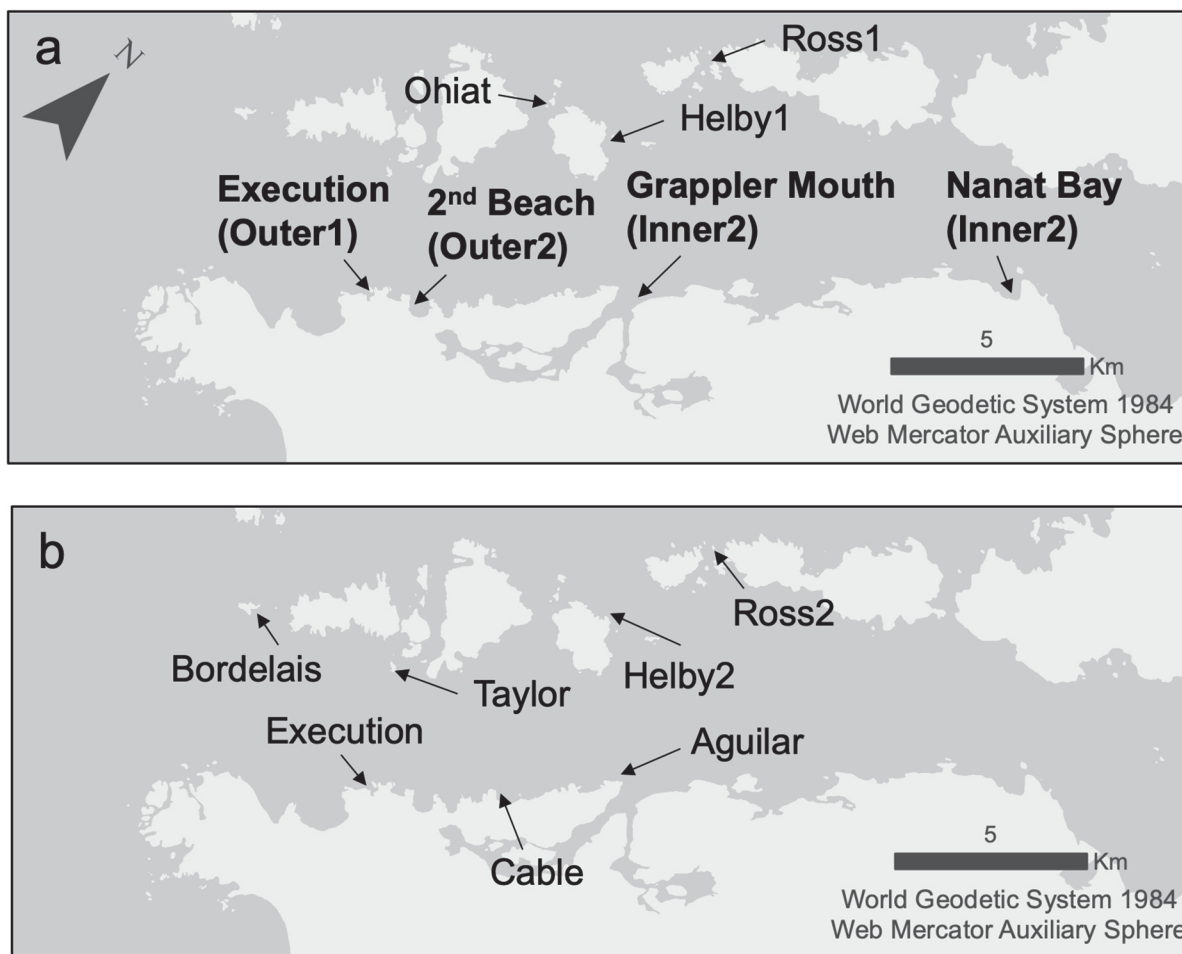


Fig. S23 Locations of growth and health studies conducted in summer 2020. Panel a shows *Macrocystis* growth (bold) and health (bold + regular text) sites; b shows *Nereocystis* health sites.

Section S1. Supplemental Methods

Section S1.1 Temperature data

We collected and compiled environmental data with two aims, first to quantify temporal changes in environmental drivers at a broad scale, and second to assess how variation in these variables is distributed across Barkley Sound. To accomplish our first goal, we compiled i) daily sea surface temperature measurements from Amphitrite Lighthouse at the outer edge of Barkley Sound (available through BC Lightstation Data Portal: <https://www.dfo-mpo.gc.ca/science/data-donnees/lightstations-phanes/index-eng.html>), and ii) temperature measured at two long-term monitoring sites: Taylor Islet and Wizard Islet (survey methods described in Watson and Estes 2011).

Our second aim was to capture spatial variation in temperature to better understand heterogeneity in the environment over which broad scale changes are superimposed. To characterize spatial variation in temperature across Barkley Sound, we deployed a series of temperature sensors across the broader region. In June – August 2019, we deployed iButton temperature loggers at 1m above chart datum at sites ($n = 22$) of varying distance from the mouth of Barkley Sound in the summer of 2019 and analyzed ~7 weeks of data collected by these loggers. Loggers were deployed by clearing a space on the rock and then cementing with Z-Spar Splashzone epoxy (West Marine Ltd., California, USA). We extracted daily mean SST by using observations from times of the day when these loggers were predicted to be completely submerged (specifically, when tidal prediction exceeded 2 metres). Thus, measurements used were taken at depths ranging from 1 to ~2.5m below the surface. In order to better characterize how temperature varies with depth, we also deployed anchored buoys ($n = 5$) in 8–12 m with temperature loggers attached. Four of these buoys were deployed for three days in August 2020 with loggers at 0.1, 2, 4, 6, and 8 metres depth to capture variation in temperature vertically in the water column. One of these buoys was deployed for ~3 weeks with a logger at 0.1m below the surface and another at 1m above the benthos. We also compared iButton temperature logger data collected at two inshore sites (Ross Islets and Fleming Island) by B. Iwabuchi and L. Gosselin (Iwabuchi and Gosselin 2019) to daily temperature measurements taken at Amphitrite Point Lighthouse on the outer coast of Barkley Sound from the summers of 2015–2016. iButton loggers were deployed at 1.5m tidal height; using tide observations from Bamfield, we extracted temperature data from when each logger was submerged below 1 – 1.5m of water to ensure only water measurements were used in the analysis.

Section S1.2 Nutrient data

To assess spatial variation in dissolved nitrate, we compared samples from two time points (Jul/Aug 1979–1982 and Aug 2021). Samples from 1979–1982 were collected and analysed using the methods described in Dreuel (1988) but have remained unpublished (now available at doi: 10.5281/zenodo.6397743). Samples collected in 2021 were immediately frozen at -20°C and remained frozen until the analysis. Samples were analysed by the Institute of Ocean Sciences in Sidney, British Columbia (Fisheries and Oceans Canada). Due to methodological limitations, we combined nitrate and nitrite concentrations into a single metric although we note that nitrate was always greater than nitrite where both variables were available (which was always <1 uM) for every sample.

Section S1.3 Urchin, seastar and subtidal kelp abundance

To assess changes in the ecosystem dynamics of subtidal kelp forests (below ~5m) during the 2014-2016 MHW, we analyzed data collected by the Parks Canada Pacific Rim National Park Reserve Dive Team. Collection of these data was led by one of the authors, J.Yakimishyn. Six subtidal sites were established throughout the Broken Group Islands and the density of *Macrocystis* kelp, red sea urchins (*Mesocentrotus fransiscanus*) and *Pycnopodia* seastars were recorded along 30m transects. Kelp stipe counts were measured in 1m² quadrats at 2m increments along the transect. *Mesocentrotus* and *Pycnopodia* abundances were measured by counting individuals along two-dimensional belt transects (2m wide x 30m long). During each survey, two transects were completed per site and sites were generally visited twice within a given year (August – September).

Section S1.4 Characterizing changes in kelp distributions (extended)

Imagery data were incorporated by using a shoreline segment method (see below). Site-level survey data were incorporated directly by conducting *in situ* resurveys of those same sites and with the same methodology. Historical maps were not treated quantitatively due to uncertainty in the spatial scale and rigour with which surveys were conducted, or because they did not cover a wide enough geographical area within Barkley Sound and/or lacked sufficient sample size for statistical analysis. However, each of these resources acted as additional sources of evidence and were qualitatively compared to other time points.

Section S1.5 Assigning and resurveying shoreline segments

In order to compare kelp distributions between 2007 ShoreZone flyover images, 1981 and 2014 aerial images, 2013 and 2016 satellite images, and *in situ* resurveys, we divided the shoreline on the southeastern wall of Barkley Sound (Fig S1) into 30-100m shoreline segments that were based off of shoreline features that were recognizable both from imagery and from a boat. These segments had a mean length of 32m and 97% were between 25 and 40 m in length. However, some large stretches of homogenous coast (e.g., beaches) were not split into shorter units due to potential uncertainty in GPS measurements that would otherwise have marked the boundary between units. Within each shoreline unit, we noted whether kelp was present or absent. For *in situ* surveys and ShoreZone aerial images, we were able to distinguish species. For satellite images and aerial imagery from higher elevations, species identification was not possible due to coarser resolution. For all imagery-based shoreline classification, segments that were not covered or were ambiguous due to glint, shadow or waves were excluded from analyses. Thus, sample sizes vary by comparison (Table S2).

Section S1.6 Resurveys of site-level data

We resurveyed three types of site-level data from two different time points. Between 1993 and 1995, Druehl and Elliot (1996) conducted a set of inventory surveys for kelp in Barkley Sound. They visited a range of intertidal and subtidal sites and documented the species present. They conducted two types of surveys, one restricted to the intertidal zone and one that included the subtidal zone. We relocated these sites using descriptions, photos and coordinates (Starko et al. 2019) and conducted resurveys following the same methods as the original surveyors. Because *Macrocystis* in Barkley Sound generally extends from the intertidal zone into the shallow subtidal zone, we considered both intertidal and subtidal data for this species. Intertidal surveys were conducted on 20–50 m stretches of coastline and included the entire intertidal region, from

Canadian datum (mean lower low water large tide - MLLWLT) to the upper limit of marine organisms. Subtidal surveys were conducted by identifying the region described by the original surveyors, which often included a photograph and a maximum depth and then identifying kelp species present from the surface. Although a coarse categorical abundance metric was used in each survey, we include only presence-absence data in this study. Given the low sample sizes of subtidal surveys (17 sites), we did not quantitatively test changes in kelp distribution but present these findings visually in Fig S10.

Section S1.7 Kelp growth measurements and condition assessments

In order to infer whether kelp in locally warm areas were physiologically stressed in shallow waters, we measured growth of tagged *Macrocystis* plants along the environmental gradient and also measured various health metrics of both *Macrocystis* and *Nereocystis* believed to be indicative of stress. In order to measure growth, we identified beds ($n = 6$) across the environmental gradient and haphazardly tagged non-terminal fronds that had obvious, active apical meristems (see Stephens 2017) using brightly coloured flagging tape. For *Macrocystis*, we tied the tape to the base of the pneumatocyst on the third disconnected blade and measured the distance to the tip of the apical meristem. We also measured the length of this blade. We then returned to these tagged kelp 6-8 days later and remeasured these values. For comparison, all growth values were standardized to change in length per day. To minimize the potentially confounded effects of water motion by waves and currents, we only selected beds in sheltered bays (see Fig S22 for locations). In order to measure the influence of this gradient on kelp health and condition, we collected individuals from beds (*Macrocystis*: $n = 5$, *Nereocystis*: $n = 6$) along the environmental gradient. For *Nereocystis*, we measured the maximum blade length and the mean length of five blades haphazardly selected from the pneumatocyst (to avoid biasing for longer or shorter blade). For *Macrocystis*, we measured an index of blade bleaching by photographing blades on a light table in a windowless room (using a Nikon D90 digital camera) and extracting a measure of darkness (as a proxy for pigmentation). All photographs were taken at a standard ISO, aperture and shutter speed and included a grey standard for reference. As an index of bleaching, we selected a uniform 5 cm diameter circle located approximately 4-5 cm from the base of each blade and calculated mean grey value from the greyscale image using ImageJ.

Section S1.8 Subtidal photoquadrat surveys

To test for an association between urchin abundance and substrate type, we measured the density of urchins and benthic substrate cover at sites along the SE wall of Barkley Sound using photo quadrats. Because urchins are known to aggregate at the edge of kelp forests, we only conducted these surveys where kelp forests were present. We tested for a relationship between urchin density and percent unconsolidated sediment (i.e., sand, sediment and cobble) using a linear model. In order to confirm whether urchin presence sets the lower limit of benthic macroalgae more generally, we also conducted vertical surveys with subtidal photo quadrats at sites north of Bamfield ($n = 8$). All photoquadrats were taken by mounting a GoPro Hero 5 to a 1m x 1m quadrat and dropping it from the boat at various depths and were conducted in Aug 2019 and Jul 2020.

Section S2. Supplemental Results and Discussion

Section S2.1 Submerged *Macrocystis* forests versus canopy-die back

We found subsurface *Macrocystis* forests at inshore sites that had locally warm surface waters. At some sites (see below), this pattern appeared to reflect upright, floating canopies that have died back from the surface. This is similar to patterns documented near the southern range edge of *Macrocystis*, where die-back from the surface can occur during strong El Nino years (Ladah et al. 1999). In other areas, especially deeper areas (below 7-8m depth), we found forests that were largely prostrate, lying flat along the bottom and reaching no more than 1-2m off of the substrate. These forests were found on mixed sand-cobble substrate that largely lacked urchins (Fig 4). These “prostrate” *Macrocystis* beds have been described previously and are more visible in the winter due to upright fronds produced by some individuals that may die back seasonally at the most inshore sites that we resurveyed (Druehl 1978). This suggests that kelp in the surface waters far from the outer coast have historically lived close to their physiological limits. It remains unclear whether prostrate fronds are an adaptation to avoid locally stressful surface waters or reflect a plastic morphological response to low water motion. Nonetheless, these prostrate fronds largely enable kelp to avoid warm surface conditions, likely enabling long-term persistence of these forests as surface waters warm.

Section S2.2 Evidence of kelp loss in the absence of urchins

While both urchins and locally warm microclimates were generally required to see complete extinction of kelp forests in our system, we documented a few instances where kelp forests have disappeared without clear evidence of urchin overgrazing. First, comparison to intertidal surveys conducted between 1993-1995 reveal that *Macrocystis* extinctions have occurred into the intertidal zone (Fig S10A). Given that urchins were always found below chart datum in our ROV surveys, we conclude that these losses were not driven by urchin grazing. Losses of other intertidal kelp were previously documented from these sheltered inshore sites, including species that extend even higher on the shore than *Macrocystis* (Starko et al. 2019).

Second, during haphazard ROV surveys, we identified multiple areas where shallow subtidal kelp forests have disappeared but leaving no clear urchin barrens. The canopy-forming forests in these areas have been replaced by understory kelp beds (e.g., *Neoagarum fimbriatum*, *Saccharina latissima*) or other seaweeds (e.g., *Sargassum*, *Desmarestia*). Although urchins are abundant in Barkley Sound and therefore we cannot fully rule out past movement of urchins into these areas, dense cover of non-canopy-forming kelp suggests that urchin grazing pressure is not sufficient to prevent kelp forest persistence and/or recovery. We therefore interpret these transitions as direct consequences of physiologically stressful surface waters. At one site (site 1 below), a drastically reduced *Macrocystis* forest remains, however no individuals reach the surface and plants show clear signs of die-back. Below we describe three of these sites in detail that experienced kelp loss without urchins.

Between Roquefoil Bay and Danver’s Point (Site 1): We conducted two haphazard ROV surveys in a small bay north of Roquefoil Bay. This region had near complete kelp forest extinction according to our surveys. While much of this stretch of coastline is rocky, this small bay is sandy which could potentially limit urchin influence. In both surveys, we did not observe urchins in this bay and instead captured mostly understory kelp beds. A small patch of

Macrocystis was found by one transect which had short or absent blades, did not reach the surface and were apparently bleaching, suggesting die back from the surface due to physiological stress.

North side of Dixon Island (Site 2): Substrate on the backside of Dixon Island is largely made up of sand, cobble and boulder, transitioning into rocky bench in the intertidal or very shallow subtidal zone. We conducted three ROV transects (one random, two haphazard) in this area. We only detected one localized patch of urchins found amongst a group of boulders. In all other cases, we did not observe any urchins. In one transect, *Macrocystis* plants were found below depths of 5m and had the submerged, prostrate form. None reached higher than ~1.5-2 m from the substrate. Historical imagery clearly shows canopy forming *Macrocystis* in shallows, reaching the surface and fringing the shoreline. However, the upright portion of this forests appears to have disappeared without clear urchin influence.

East side of Fleming Island (Site 3): We conducted multiple haphazard surveys in a bay on the east side of Fleming Island that revealed a mosaic of urchin barrens and understory kelp beds (i.e., *Neoagarum*, *Saccharina*) on sand and cobble. In Fig S20, we show how while an offshore reef that previously had kelp has been replaced with a barren, portions of the former forest closer to shore lack urchins and are now prostrate kelp beds growing on cobble in sand. During one of these surveys, we detected a handful of *Nereocystis* individuals that were not at the surface (in October) and appeared to be in very poor health (short, bleached blades; Fig S22). The shallow subtidal zone across this site are dominated by understory kelp, *Desmarestia* spp., and *Sargassum muticum*.

Section S3. Supplemental References

- Druehl, L. D. 1978. The distribution of *Macrocystis integrifolia* in British Columbia as related to environmental parameters. *Canadian Journal of Botany* 56:69–79.
- Druehl, L. D., R. Baird, A. Lindwall, K. E. Lloyd, and S. Pakula. 1988. Longline cultivation of some Laminariaceae in British Columbia, Canada. *Aquaculture Research* 19:253–263.
- Iwabuchi, B. L., and L. A. Gosselin. 2019. Long-term trends and regional variability in extreme temperature and salinity conditions experienced by coastal marine organisms on Vancouver Island, Canada. *Bulletin of Marine Science* 95:337–354.
- Ladah, L. B., J. A. Zertuche-González, and G. Hernández-Carmona. 1999. Giant Kelp (*Macrocystis pyrifera*, Phaeophyceae) Recruitment Near Its Southern Limit in Baja California After Mass Disappearance During Enso 1997–1998. *Journal of Phycology* 35:1106–1112.
- Starko, S., L. A. Bailey, E. Creviston, K. A. James, A. Warren, M. K. Brophy, A. Danasel, M. P. Fass, J. A. Townsend, and C. J. Neufeld. 2019. Environmental heterogeneity mediates scale-dependent declines in kelp diversity on intertidal rocky shores. *PLOS ONE* 14:e0213191.
- Stephens, T. A. 2017. Terminal blades in *Macrocystis* and their unexplored links to functional biology. *Ecology* 98:2727–2729.
- Watson, J., and J. A. Estes. 2011. Stability, resilience, and phase shifts in rocky subtidal communities along the west coast of Vancouver Island, Canada. *Ecological Monographs* 81:215–239.